

Evaluation of the effects of shaking intensity on the process of methylene blue discoloration by metallic iron

Noubactep C.*, Kurth A.-M.F., Sauter M.

Angewandte Geologie, Universität Göttingen, Goldschmidtstraße 3, D - 37077 Göttingen, Germany.

* Corresponding author: e-mail: cnoubac@gwdg.de; Tel. +49 551 39 3191, Fax: +49 551 399379

Abstract

The term mixing (shaking, stirring, agitating) is confusing because it is used to describe mass transfer in systems involving species dissolution, species dispersion and particle suspension. Each of these mechanisms requires different flow characteristics in order to take place with maximum efficiency. This work was performed to characterize the effects of shaking intensity on the process of aqueous discoloration of methylene blue (MB) by metallic iron (Fe^0). The extent of MB discoloration by three different materials in five different systems and under shaking intensities varying from 0 to 300 min^{-1} was directly compared. Investigated materials were scrap iron (Fe^0), granular activated carbon (GAC), and deep sea manganese nodules (MnO_2). The experiments were performed in essay tubes containing 22 mL of the MB solution (12 mg/L or 0.037 mM). The essay tubes contained either: (i) no reactive material (blank), (ii) 0 to 9.0 g/L of each reactive material (systems I, II and III), or (iii) 5 g/L Fe^0 and 0 to 9.0 g/L GAC or MnO_2 (systems IV and V). The essay tubes were immobilized on a support frame and shaken for 0.8 to 5 days. Non-shaken experiments lasted for duration up to 50 days. Results show increased MB discoloration with increasing shaking intensities below 50 min^{-1} , a plateau between 50 and 150 min^{-1} , and a sharp increase of MB discoloration at shaking intensities $\geq 200 \text{ min}^{-1}$. At 300 min^{-1} , increased MB discoloration was visibly accompanied by suspension of dissolution products of Fe^0/MnO_2 and suspension of GAC fines. The results suggest that, shaking intensities aiming at facilitating contaminant mass transfer to the Fe^0 surface should not exceed 50 min^{-1} .

27 **Keywords:** Adsorption; Co-precipitation; Methylene Blue; Shaking Intensity; Zerovalent
28 Iron.

29 **Introduction**

30 The processes occurring at the interface $\text{Fe}^0/\text{H}_2\text{O}$ are of great interest for the use of metallic
31 iron in environmental remediation (e.g. in $\text{Fe}^0/\text{H}_2\text{O}$ systems). A great deal of work has been
32 reported in this area during the past 20 years [1-10]. Since the seminal work of Matheson and
33 Tratnyek [1], a substantial amount of literature concerning the removal mechanism of various
34 contaminants in $\text{Fe}^0/\text{H}_2\text{O}$ systems has been published. This is not surprising given that: (i) the
35 concept of permeable reactive barrier (PRB) is regarded as a significant advance in
36 remediation technology [11,12], and (ii) iron PRBs have been demonstrated very efficient to
37 mitigate contaminants in surface and ground waters [3-5]. Moreover, $\text{Fe}^0/\text{H}_2\text{O}$ systems have
38 been shown to effectively removed aqueous species of various nature. These include viruses
39 [13], bacteria [14], inorganics [15,16], redox-sensitive organics [1,17], and redox-insensitive
40 organics [18]. The large diversity of contaminants successfully removed in $\text{Fe}^0/\text{H}_2\text{O}$ systems
41 has recently prompted the revision of the initial "reductive transformation" concept [1,19].
42 The "reductive transformation" concept is obviously inconsistent with quantitative removal of
43 redox-insensitive species. A new concept of "adsorption/co-precipitation" was introduced
44 [20,21] stipulating that adsorption and co-precipitation are the fundamental mechanisms of
45 contaminant removal in $\text{Fe}^0/\text{H}_2\text{O}$ systems. The adsorption/co-precipitation concept is free of
46 contradictions inherent to reductive transformation concept and explains some controversial
47 experimental facts [20]. After the new concept, a $\text{Fe}^0/\text{H}_2\text{O}$ system should be regarded as a
48 zone of precipitating iron oxides. Each species (including contaminants) entering this zone
49 will be first adsorbed onto and/or co-precipitated with iron (hydr)oxides but could undergo
50 further abiotic transformations [including reduction by electrons from Fe^0 , Fe^{II} , H_2/H and
51 oxidation by Fenton reagents (Fe^{II} and H_2O_2), , which react to highly oxidizing $\cdot\text{OH}$ -radicals].

52 Regarding $\text{Fe}^0/\text{H}_2\text{O}$ systems as zones of precipitating iron oxides suggests a profound analysis
53 of the process of iron precipitation to better characterize its impact on contaminant removal
54 under given relevant conditions. The adsorption of a contaminant onto a solid/ H_2O interface
55 involves a cascade of complex events occurring almost simultaneously: (i) transport of
56 contaminant molecules from the bulk solution to the interface by diffusion or
57 diffusion/convection processes; (ii) adsorption of contaminant molecules at the solid/ H_2O
58 interface; (iii) structural modifications of the fixed molecules together for high surface
59 coverages and interactions of the incoming molecules with previously accumulated
60 contaminant molecules [22]. In real natural systems, adsorption competition between
61 molecules of different nature and molecular weight should be additionally considered.

62 The particularity of $\text{Fe}^0/\text{H}_2\text{O}$ systems is three fold: (i) Fe^0 dissolution and precipitation yields
63 a complex hydroxide and oxide mixture of unknown composition, (ii) Fe^0 and Fe^{II} are
64 potential reducing agents, and (iii) the weight fraction of iron hydroxide and oxide particles
65 increases from zero at the beginning to more or less higher proportions depending on the
66 reaction progress. The net result is a multi-solid reaction system involving many types of
67 solids of widely differing sizes and density (Fe^0 and various iron hydroxides/oxides). The
68 large changes in the solid composition during the reaction will certainly influence the mass
69 transfer of species to the $\text{Fe}^0/\text{H}_2\text{O}$ interface and thereby play a significant role in the
70 determination of reaction rates [23]. Moreover, in situ formed iron oxides are not inert with
71 regard to contaminant removal [20,21]. Therefore, the effective mass transfer to the $\text{Fe}^0/\text{H}_2\text{O}$
72 interface depends also on the affinity of iron hydroxides/oxides to the contaminants.

73 The process of iron oxide precipitation results from the hydrolysis and precipitation of
74 $\text{Fe}^{\text{II}}/\text{Fe}^{\text{III}}$ hydroxides followed by dehydration. Thereby, amorphous iron hydroxides
75 $[\text{Fe}(\text{OH})_2/\text{Fe}(\text{OH})_3]$ of very large surface areas are transformed to more crystalline oxides
76 (FeOOH , Fe_2O_3 , Fe_3O_4). The most characteristic feature is that the system undergoes an
77 irreversible process controlled by hydrodynamic and physicochemical conditions. The present

78 work mainly pay the attention to the hydrodynamic conditions. In accelerated batch
79 experiments, the reaction progress is largely dependent on the particle size of used Fe^0 and
80 mixing procedure (agitating, shaking, stirring) and mixing intensity/speed. For a system in
81 which new solid phases of various size and density are present, used mixing designs and
82 mixing intensities should be one of the major sources of reported discrepancies. In fact
83 mixing may hold original and new formed particles in suspension [24, 25], thereby disturbing
84 the natural layered disposition of Fe^0 and Fe-oxides.

85 The two objectives of this work were: (i) to characterise the effect of shaking intensity on the
86 process of methylene blue (MB) discoloration from the aqueous solution by metallic iron
87 (Fe^0), and (ii) to identify the critical shaking intensity above which the process of MB
88 discoloration by Fe^0 is significantly disturbed to be representative for natural situations. The
89 critical shaking intensity is defined as the shaking intensity above which mixing operations
90 induce more that speeding up external mass-transfer of contaminants from the bulk solution to
91 the vicinity of Fe^0 (see next section). For this purpose separate discoloration experiments were
92 performed in five different systems (i) metallic iron (system I), (ii) granular activated carbon
93 (system II), (iii) manganese nodules (system III), (iv) " $\text{Fe}^0 + \text{GAC}$ " (system IV), and (v) " Fe^0
94 + MnO_2 " (system V). The results were comparatively discussed.

95 **Background of the experimental methodology**

96 In laboratory batch experiments mixing operations are mainly used for two purposes [24, 25]:
97 (i) accelerating solid phase dissolution (process I), and (ii) accelerating mass transfer of solute
98 to a solid/liquid interface (process II). The latter aspect includes efforts to keep reactive
99 surface in suspension (process III). Depending on the aqueous chemical reactivity of the solid
100 phase and the mixing intensity, process I, II and III are more or less likely to occur. For an
101 inert solid phase as granular activated carbon (GAC) process I may not occur. But for reactive
102 solid phases (Fe^0 , MnO_2) process I through III may simultaneously occur depending on the
103 mixing intensity. With other words, in a $\text{Fe}^0/\text{H}_2\text{O}$ system mixing operations may induce at

104 least two antagonistic effects: (i) mass transfer to the $\text{Fe}^0/\text{H}_2\text{O}$ interface and (ii) accelerated
105 Fe^0 dissolution. Mass transfer to the $\text{Fe}^0/\text{H}_2\text{O}$ interface has been largely considered while
106 accelerated Fe^0 dissolution and its consequences on the process of contaminant removal have
107 been almost overseen [20,21]. Moreover, vigorous mixing can also induce two negative
108 effects: (i) breaking the material grains subject to friability (attrition) [25], and (ii) eliminating
109 the diffusion inhibition of surface processes [26]. Tomashov and Vershinina [26] have shown
110 that a sufficiently vigorous stirring and continuous renewal of the Fe^0 surface (scouring)
111 eliminates the inhibition of the electrode-process step associated with adsorption or the
112 formation of surface layers.

113 The transport of solutes in a $\text{Fe}^0/\text{H}_2\text{O}$ system proceeds in two ways: advection and diffusion.
114 Advection is caused by water flow, while diffusion is caused by the concentration gradient
115 [27,28]. Diffusion of solutes in water corresponds with the chemical reactions, if advection
116 due to the water flow is slow enough. Advection does not induce any additive process in the
117 system but speeds up processes observable when diffusion is the sole transport mechanism
118 (**Assumption 1**). Assumption 1 is the main argument on which this study is built. Thereafter,
119 results achieved in non-disturbed systems (diffusion-controlled), relevant for environmental
120 situations, should be reproducible under shaken conditions. Accordingly, relevant shaking
121 intensities for $\text{Fe}^0/\text{H}_2\text{O}$ systems should not induce further processes causing suspension of in-
122 situ generated corrosion products or abrasion of oxide films. Clearly, applied mixing
123 intensities should solely speed up external mass-transfer of contaminants from the bulk
124 solution to the vicinity of the solid.

125 **Materials and methods**

126 **Reagent and materials**

127 Methylene blue (MB) is a traditionally favourite dye of choice for laboratory and technical
128 purposes [29-31]. Its molecule has a minimum diameter of approximately 0.9 nm [31] and is
129 used as redox indicator [32]. As positively charged ions, MB should readily adsorb onto

130 negatively charged surface. That is at $\text{pH} > \text{pH}_{\text{pzc}}$; pH_{pzc} being the pH at the point of zero
131 charge [33]. The used initial concentration was 12 mg L^{-1} ($\sim 0.037 \text{ mM}$) MB and it was
132 prepared by diluting a 1000 mg L^{-1} stock solution. All chemicals were analytical grade.
133 The used Fe^0 material is a readily available scrap iron. Its elemental composition was
134 determined by X-Ray Fluorescence Analysis and was found to be: C: 3.52%; Si: 2.12%; Mn:
135 0.93%; Cr: 0.66%. The material was fractionated by sieving. The fraction 1.6 - 2.5 mm was
136 used. The sieved Fe^0 was used without any further pre-treatment.
137 The used granular activated carbon (GAC) from LS Labor Service GmbH
138 (Griesheim/Germany) was crushed and sieved. The particle sized fraction ranging from 0.63
139 to 1.0 mm was used without further characterization.
140 Manganese nodules (MnO_2) collected from the deep sea was crushed and sieved. An average
141 particle size of 1.5 mm was used. Its elemental composition was determined by X-Ray
142 Fluorescence Analysis and was found to be: Mn: 41.8%; Fe: 2.40%; Si: 2.41%; Ni: 0.74%;
143 Zn: 0.22%; Ca: 1.39%; Cu: 0.36%. These manganese nodules originated from the pacific
144 ocean (Guatemala basin: $06^\circ 30 \text{ N}$, $92^\circ 54 \text{ W}$ and 3670 m deep). The target chemically active
145 component is MnO_2 , which occurs naturally mainly as birnessite and todorokite [34].

146 **Rationale for choice of test conditions**

147 Materials selected for study were known to be effective for adsorbing MB (GAC), discoloring
148 MB (Fe^0 , MnO_2) or delaying the availability of iron corrosion products in $\text{Fe}^0/\text{H}_2\text{O}$ systems
149 (MnO_2) [35]. MB co-precipitation with in situ formed iron corrosion products was
150 demonstrated to be the main mechanism of discoloration [36].

151 Table 1 summarises the function of the individual materials and gives the material surface
152 coverage in individual reaction vessels. The detailed method for the calculation of the surface
153 coverage (θ) is presented by Jia et al. [18]. The minima of reported specific surface area
154 (SSA) values of the adsorbents were used for the estimation of surface coverage. The Fe^0 SSA
155 was earlier measured by Mbudi et al. [37]. The value 120 \AA^2 is considered for the molecular

156 cross-sectional area of MB [31]. From Tab. 1 it can be seen that, apart from Fe^0 ($\theta = 18.8$), all
157 other materials were present in excess “stoichiometry” ($\theta \leq 0.13$). This means that the
158 available surface of Fe^0 could be covered by up to 18 mono-layers of MB, whereas the other
159 materials should be covered to less than one fifth with MB ($\theta = 1$ corresponds to a mono-layer
160 coverage). Therefore, depending on the initial pH value and the affinity of MB for the
161 individual materials (pH_{pzc}) and the kinetics of MB transport to the reactive sites (material
162 porosity, shaking intensity), the MB discoloration should be quantitative for sufficient
163 experimental duration. A survey of the pH_{pzc} values given in Tab. 1 suggests that MB
164 adsorption onto all used adsorbents should be favourable because the initial pH was 7.8. At
165 this pH value all surfaces are negatively charged; MB is positively charged. Because the
166 available Fe^0 surface can be covered by up to 18 layers of MB, a progressive MB
167 discoloration in presence of Fe^0 is expected.

168 **Discoloration studies**

169 Batch experiments with shaking intensities varying from 0 to 300 min^{-1} were conducted in
170 essay tubes for experimental durations varying from 0.83 to 50 days. The essay tubes were
171 immobilized on a support frame and shaken for 0.8 to 7 days. A rotary shaker HS 501 D from
172 “Janke & Kunkel”, DCM Laborservice, with a maximum shaking intensity of 300 min^{-1} was
173 used. A non-disturbed experiment was conducted for 25 and 50 days. The batches consisted
174 of 0 to 9.0 g L^{-1} of a material (GAC, Fe^0 , MnO_2 systems I, II and III) or $5 \text{ g L}^{-1} \text{ Fe}^0$ and 0 to
175 9.0 g L^{-1} GAC (system IV) and MnO_2 (system V) respectively. A reaction time of 25 d for the
176 non-disturbed experiment was selected to allow a MB discoloration efficiency of about 80%
177 in the system with Fe^0 alone. The experiment with 50 d reaction time targeted a better
178 characterization of system V ($\text{Fe}^0 + \text{MnO}_2$). The extent of MB discoloration in the five
179 systems was characterized under various shaking intensities. For this purpose 0.0 to 0.20 g of
180 Fe^0 and the additives were allowed to react in sealed sample tubes containing 22.0 mL of a
181 MB solution (12 mg L^{-1}) at laboratory temperature (about 20° C). Initial pH was ~ 7.8 . After

182 equilibration, up to 3 mL of the supernatant solutions were carefully retrieved (no filtration)
183 for MB measurements (no dilution). In the experiments at shaking intensities $> 150 \text{ min}^{-1}$ the
184 samples were centrifuged at 5000 min^{-1} for 20 min prior to spectrophotometric analysis [38].

185 **Analytical methods**

186 MB concentrations were determined by a Cary 50 UV-Vis spectrophotometer (Varian) at a
187 wavelength of 664.5 nm using cuvettes with 1 cm light path. The pH value was measured by
188 combined glass electrodes (WTW Co., Germany). Electrodes were calibrated with five
189 standards following a multi-point calibration protocol in agreement with the current IUPAC
190 recommendation [39].

191 Each experiment was performed in triplicate and averaged results are presented.

192 **Results and Discussion**

193 After the determination of the residual MB concentration (C) the corresponding percent MB
194 discoloration was calculated according to the following equation (Eq. 1):

$$195 \quad P = [1 - (C/C_0)] * 100\% \quad (1)$$

196 where C_0 is the initial aqueous MB concentration (about 12 mg L^{-1}), while C gives the MB
197 concentration after the experiment. The operational initial concentration (C_0) for each case
198 was acquired from a triplicate control experiment without additive material (so-called blank).
199 This procedure was to account for experimental errors during dilution of the stock solution,
200 MB adsorption onto the walls of the reaction vessels and all other possible side reaction
201 during the experiments.

202 **Evidence for the effect of shaking on the process MB discoloration**

203 Preliminary qualitative experiments at 300 min^{-1} showed that the MB solution in the assay
204 tubes in all systems became very turbid due to particle attrition (breaking the grains of GAC,
205 MnO_2) or suspension of in-situ generated iron oxides (Fig. SC1 – supplementary Content). In
206 systems IV and V (see table 2), suspended iron oxides may compete with MB for adsorption
207 site on GAC or MnO_2 . Attrition of GAC and MnO_2 certainly increases the surface area of the

208 adsorbents, accelerating the MB adsorption kinetics. Keeping in mind that relevant mixing
209 operations should solely provide a uniform distribution of the MB in the solution
210 (Assumption 1), further experiments targeted at better characterizing the effects of shaking
211 intensity on the process of MB discoloration.

212 **Effects of the shaking intensity on the MB discoloration in investigated systems**

213 Figure 1 compares the extent of MB discoloration in the five investigated systems as the
214 shaking intensity varies from 0 to 300 min⁻¹ for an experimental duration of 24 h (1 d).

215 The observed general trend can be summarized as follows: (i) shaking at 50 min⁻¹
216 significantly increases the extent of MB discoloration in all systems comparatively to non-
217 disturbed experiments; (ii) increasing the shaking intensity from 50 to 200 min⁻¹ has no
218 significant effect on MB discoloration (except for system II); (iii) increasing the shaking
219 intensity from 200 to 300 min⁻¹ resulted in total MB discoloration for all systems except
220 system I.

221 Interestingly, the expected lower MB discoloration in system V relative to system I could not
222 be observed at all tested shaking intensity for 1 d. In other words, the well-documented
223 reductive dissolution of MnO₂ by Fe^{II} [40,41] could not be observed. Therefore, shaking
224 operations definitively significantly influences the mechanism of contaminant removal in
225 Fe⁰/H₂O systems.

226 The increased discoloration efficiency of system II at 200 min⁻¹ comparatively to system IV
227 suggests that suspended corrosion products have impaired MB discoloration by competing for
228 GAC adsorption sites. Accordingly, fines from GAC which are responsible for increased
229 discoloration at a shaking intensity of 200 min⁻¹ in system II are (at least partly) covered by
230 suspended corrosion products in system IV yielding lower MB discoloration. At 300 min⁻¹
231 enough fine are present for total MB discoloration despite the inhibitory effects of suspended
232 corrosion products. The fact that MB discoloration was the lowest in system I (Fe⁰ alone) is
233 consistent with the hypothesis of discoloration inhibition by suspended corrosion products.

234 With regards on the mechanism of MB discoloration [36] it should be considered that
235 suspended corrosion products are kept in the solution and their polymerisation is impaired
236 yielding low precipitation and thus, low extent of MB co-precipitation.

237 The fact that the well documented impact of MnO_2 on the process of MB discoloration (MB
238 co-precipitation) by Fe^0 could not be experimentally observed could suggest that, for a mass
239 of 5 g/l, a reaction time of 1 day was too short (**Assumption 2**). Before testing the validity of
240 assumption 2, the results of shaken experiments for 5 days should first be presented and
241 compared to that of non-disturbed experiments for 25 days. Kurt [38] demonstrated increased
242 MB discoloration with increased shaking time.

243 **Effects of shaking intensity on the kinetics of MB discoloration**

244 Figure 2 compares the extent of MB discoloration as function of material loading in systems I,
245 II and III under non-disturbed conditions for 25 days (Fig. 2a) and at a shaking intensity of
246 150 min^{-1} for 5 days (Fig. 2b). The results showed that under non-disturbed conditions less
247 than 60 % of the initial amount of MB could be discoloured in all systems and Fe^0 was the
248 most efficient material (58 %). The order of increasing discoloration efficiency was $\text{MnO}_2 <$
249 $\text{GAC} < \text{Fe}^0$. At mass loadings $\geq 8 \text{ g/L}$ the discoloration efficiency of GAC and Fe^0 were very
250 comparable. This observation can be explained by the porous nature of GAC: slow intra-
251 particle diffusion [25].

252 Under shaken conditions, Fe^0 was clearly the less efficient material and its maximal
253 discoloration efficiency was 50 %. This result confirms that shaking is somehow inhibiting for
254 the process of MB discoloration. The discoloration efficiency for MnO_2 and GAC was larger
255 than 60 %. The order of increasing discoloration efficiency was $\text{Fe}^0 < \text{MnO}_2 < \text{GAC}$. It is
256 important to note that: (i) MB discoloration was completed in the presence of GAC for mass
257 loadings $> 5 \text{ g L}^{-1}$, and (ii) in all the systems a plateau was observed for loadings $> 4.5 \text{ g L}^{-1}$.
258 This plateau corresponds to slow processes that can not be significantly accelerated under the
259 experimental conditions (150 min^{-1} , 5 days). This conclusion is supported by the fact that an

260 higher discoloration efficiency could be observed under non-disturbed conditions with Fe^0 for
261 25 days. As all materials were at the bottom of the assay tubes a slow process common to all
262 systems can be inter-particle MB diffusion to the material (re)active sites. For Fe^0 additional
263 slow processes are the oxidative dissolution of Fe^0 (chemical reaction) and the MB diffusion
264 across the oxide film on Fe^0 surface [23]. For MnO_2 the additional slow process can be the
265 reductive dissolution (yielding Mn^{II} species) or MB intra-particle diffusion to the reactive site.
266 For porous GAC possible slow processes are MB inter-particle and intra-particle diffusion.
267 Figure 2 clearly shows that shaking accelerates the kinetics of MB transport to the surface of
268 GAC and MnO_2 yielding higher discoloration efficiency relative to non-disturbed systems.
269 Thereby GAC is always more efficient than MnO_2 . Therefore, assumption 1 is verified for
270 GAC and MnO_2 . As concerning the system with Fe^0 , it is obvious that shaking the system for
271 at 150 min^{-1} for 5 days was not sufficient to achieved more than 50 % MB discoloration .
272 These results may suggest either that (i) iron corrosion was too slow to produce enough
273 corrosion products for MB co-precipitation, (ii) the kinetics of corrosion products
274 precipitation was too high to induce quantitative MB co-precipitation, or (iii) in-situ formed
275 corrosion products are kept suspended in the solution (co-precipitation occurs to a lesser
276 extent). To bring more clarity in this issue, the effect of MnO_2 on MB discoloration by Fe^0
277 (systems I and V) in non-disturbed experiments and experiments at 150 min^{-1} for 5 days were
278 compared.

279 **Effects of shaking intensity on MB discoloration in $\text{Fe}^0/\text{MnO}_2/\text{H}_2\text{O}$ systems**

280 Figure 3 compares the extent of MB discoloration as function of material loading in systems I,
281 III and V under non-disturbed conditions for 25 days (Fig. 3a) and at a shaking intensity of
282 150 min^{-1} for 5 days (Fig. 3b). The results of systems I and III have already been discussed
283 (Fig. 2). This section will focus on system V to test the validity of assumption 2.

284 Figure 3a clearly shows that under non-disturbed conditions, MB discoloration is inhibited in
285 the presence of MnO_2 as expected. However, this inhibition is limited to low MnO_2 mass

286 loadings (≤ 4.5 g/l). The initial discoloration efficient of 48 % at 0 g/l MnO_2 decreases to 13
287 % at 1.1 g/l MnO_2 and then increases with increasing MnO_2 mass loading. The fact that the
288 discoloration efficiency at MnO_2 mass loading > 4.5 g/l was higher than in both system I and
289 system III (Fig. 3a) suggests that MB serves as redox indicator [32] to evidence extensive
290 oxidation of Fe^{II} to Fe^{III} in the presence of large amounts of MnO_2 . Because the experiments
291 were performed under oxic conditions, the observed reducing conditions should be regarded
292 as a transition state afterwards the colorless Leuco-Methylene Blue (LMB) is backwards
293 oxidized to MB by diffused molecular oxygen. Note that, in his experiments for 35 days using
294 20 mg/l MB and the same experimental conditions, Noubactep [36] could not observed the
295 redox indicator properties of MB but a slight further decrease of MB discoloration with
296 increasing MnO_2 mass loading. The redox indicator properties of MB was also not observed
297 in shaken experiments (Fig. 3b). Hence, the merit of non-disturbed experiments to evidence
298 theoretically foreseeable processes [42] is underlined here.

299 Figure 3b shows no significant effect of MnO_2 on the process of MB discoloration by Fe^0 . It
300 can be seen that the extent of MB discoloration remains constant to approximately 40 %
301 when the MnO_2 loading increases from 0 to 9 g/l. Therefore, assumption 2 is not verified,
302 showing that shaking disturbs the process of iron precipitation and thus the process of MB co-
303 precipitation with iron corrosion products. On the other side, the redox indicator properties of
304 MB are not also evidenced as discussed above.

305 Figure 4 compares the MB discoloration efficiency in system V after 25 and 50 days. It is
306 very interesting to see that for sufficient long experimental duration (50 d), MB discoloration
307 is quantitative for all MnO_2 loadings (≤ 9.1 g/l). This result corroborates the ability of non-
308 disturbed experiments to evidence theoretically foreseeable processes. Accordingly mixing
309 operation may accelerate investigated process in such a way that important aspects are
310 overseen. Two examples could be given in this study: (i) the well-documented redox indicator

311 properties of MB [32], and (ii) the reductive dissolution of MnO_2 inducing delay in the
312 availability of free corrosion products for MB co-precipitation [36].

313 **Conclusions**

314 The effects of shaking intensity on the process of MB discoloration was characterized in a
315 sequence of experiments. The working hypothesis was that any relevant mixing operation for
316 real world situations should solely accelerate the diffusive transport of MB from the aqueous
317 solution to the interface solid/ H_2O . The results indicated that shaking intensities $\geq 50 \text{ min}^{-1}$
318 lead to a suspension of in-situ generated iron corrosion products and to a delay of the process
319 of MB co-precipitation. More importantly, apart from non-disturbed systems, none of the
320 tested experimental conditions could reproduce the well-documented reductive dissolution of
321 MnO_2 by Fe^{II} species [40,41] which would have been reflected by a delay in MB co-
322 precipitation by Fe^0 in the presence of MnO_2 . Finally, non-disturbed experiments could
323 evidence the well-documented redox indicator properties of MB. Mixing intensity $< 50 \text{ min}^{-1}$
324 were not tested, but the complexity of mixing operations on processes in $\text{Fe}^0/\text{H}_2\text{O}$ systems
325 could be unambiguously evidenced. Generally, the mixing intensity is considered of utmost
326 importance when it leads to attrition of the reactive media [25]. However, even this aspect is
327 not usually taken into account in most studies, and mixing intensities higher than 300^{-1} min
328 have been used in characterising redox processes in $\text{Fe}^0/\text{H}_2\text{O}$ systems [43,44].

329 **Implication for future works**

330 As part of any proposed process, the fundamentals of the reaction need to be investigated to
331 aid in the optimisation of the process [1,45]. The present work has unambiguously shown the
332 influence of shaking intensity on the process of contaminant removal in $\text{Fe}^0/\text{H}_2\text{O}$ systems on
333 the example of methylene blue discoloration by metallic iron (Fe^0). It can be expected that
334 other mixing procedures (stirring, agitating, vortex) have similar disturbing impacts. These
335 disturbing impacts are yet to characterise and consider for further technology development.

336 The results of the present work have shown that, while using mixing operations as a tool to
337 accelerate the reaction kinetics and achieve elevated removal efficiencies within relative short
338 times, a severe bias was introduced. The net effect of elevated mixing intensities is two fold:
339 (i) to inhibit the precipitation of iron oxides in the vicinity of Fe^0 by favouring the transport
340 of Fe^{II} and Fe^{III} species away from the Fe^0 surface, and (ii) to sustain suspension of initial
341 corrosion products and delay quantitative precipitation.

342 Given the large diversity of mixing devices used in experiments for contaminant removal in
343 $\text{Fe}^0/\text{H}_2\text{O}$, the critical value of 50 min^{-1} given in this work has only an indicative value. For any
344 mixing device preliminary investigations should help to identify the domain of mixing
345 intensities for which mixing can be considered to facilitate contaminant transport to the
346 interface $\text{Fe}^0/\text{H}_2\text{O}$ without substantially disturbing the process of iron oxide precipitation. In
347 general, experiments pertinent to subsurface $\text{Fe}^0/\text{H}_2\text{O}$ systems should not be performed under
348 shaking conditions higher than the groundwater flowing velocities.

349 Repeating reported experiments with several organic and inorganic compounds exhibiting
350 various (i) redox reactivity, (ii) molecular sizes and (iii) affinity for iron oxides will enable a
351 better comprehension of the influence of shaking on the process of contaminant removal for
352 environmental remediation.

353 **Acknowledgments**

354 For providing the iron material investigated in this study the authors would like to express
355 their gratitude to the branch of the MAZ (Metallaufbereitung Zwickau, Co) in Freiberg
356 (Germany). Mechthild Rittmeier, Florian Deisinger and Gerhard Max Hundertmark are
357 acknowledged for technical support. The work was granted by the Deutsche
358 Forschungsgemeinschaft (DFG-No 626/2-2).

359 **Supplementary Content:** Photographic documentation of turbid systems as results of
360 shaking at 300 min^{-1} for 1 and 3 d.

361 **References**

- 362 [1] L.J. Matheson, P.G. Tratnyek, Reductive dehalogenation of chlorinated methanes by iron
363 metal, *Environ. Sci. Technol.* 28 (1994), 2045-2053.
- 364 [2] S.F. O'Hannesin, R.W. Gillham, Long-term performance of an in situ "iron wall" for
365 remediation of VOCs. *Ground Water* 36 (1998), 164-170.
- 366 [3] J.L. Jambor, M. Raudsepp, K. Mountjoy, Mineralogy of permeable reactive barriers for
367 the attenuation of subsurface contaminants. *Can. Miner.* 43 (2005), 2117-2140.
- 368 [4] A.D. Henderson, A.H. Demond, Long-term performance of zero-valent iron permeable
369 reactive barriers: a critical review. *Environ. Eng. Sci.* 24 (2007), 401-423.
- 370 [5] D.F. Laine, I.F. Cheng, The destruction of organic pollutants under mild reaction
371 conditions: A review. *Microchem. J.* 85 (2007), 183-193.
- 372 [6] A.B. Cundy, L. Hopkinson, R.L.D. Whitby, Use of iron-based technologies in
373 contaminated land and groundwater remediation: A review. *Sci. Tot. Environ.* 400 (2008), 42-
374 51.
- 375 [7] R.L. Johnson, R.B. Thoms, R.O'B. Johnson, T. Krug, Field evidence for flow reduction
376 through a zero-valent iron permeable reactive barrier. *Ground Water Monit. Remed.* 28
377 (2008), 47-55.
- 378 [8] R.L. Johnson, R.B. Thoms, R.O'B. Johnson, J.T. Nurmi, P.G. Tratnyek, Mineral
379 precipitation upgradient from a zero-valent iron permeable reactive barrier. *Ground Water*
380 *Monit. Remed.* 28 (2008), 56-64.
- 381 [9] J. Suk O, S.-W. Jeon, R.W. Gillham, L. Gui, Effects of initial iron corrosion rate on long-
382 term performance of iron permeable reactive barriers: Column experiments and numerical
383 simulation. *J. Contam. Hydrol.* 103 (2009), 145-156.
- 384 [10] R. Thiruvengkatachari, S. Vigneswaran, R. Naidu, Permeable reactive barrier for
385 groundwater remediation. *J. Ind. Eng. Chem.* 14 (2008), 145-156.

- 386 [11] D.C. McMurty, R.O. Elton, New approach to in-situ treatment of contaminated
387 groundwaters. *Environ. Progr.* 4/3 (1985), 168-170.
- 388 [12] R.C. Starr, J.A. Cherry, In situ remediation of contaminated Ground water: The funnel-
389 and-Gate System. *Ground Water* 32 (1994), 465-476.
- 390 [13] Y. You, J. Han, P.C. Chiu, Y. Jin, Removal and inactivation of waterborne viruses using
391 zerovalent iron. *Environ. Sci. Technol.* 39 (2005), 9263-9269.
- 392 [14] A. Hussam, A.K.M. Munir, A simple and effective arsenic filter based on composite iron
393 matrix: Development and deployment studies for groundwater of Bangladesh. *J. Environ. Sci.*
394 *Health A* 42 (2007), 1869-1878.
- 395 [15] D.W. Blowes, C.J. Ptacek, S.G. Benner, W.T. Mcrae Che, T.A. Bennett, R.W. Puls,
396 Treatment of inorganic contaminants using permeable reactive barriers. *J. Contam. Hydrol.* 45
397 (2000), 123-137.
- 398 [16] K.J. Cantrell, D.I. Kaplan, T.W. Wietsma, Zero-valent iron for the in situ remediation of
399 selected metals in groundwater. *Journal of Hazardous Materials* 42 (1995), 201-212.
- 400 [17] R. Miehr, G.P. Tratnyek, Z.J. Bandstra, M.M. Scherer, J.M. Alowitz, J.E. Bylaska,
401 Diversity of contaminant reduction reactions by zerovalent iron: Role of the reductate.
402 *Environ. Sci. Technol.* 38 (2004), 139-147.
- 403 [18] Y. Jia, Aagaard P., Breedveld G.D, Sorption of triazoles to soil and iron minerals,
404 *Chemosphere* 67 (2007) 250-258.
- 405 [19] E.J. Weber, Iron-mediated reductive transformations: investigation of reaction
406 mechanism. *Environ. Sci. Technol.* 30 (1996), 716-719.
- 407 [20] C. Noubactep, Processes of contaminant removal in “Fe⁰-H₂O” systems revisited: The
408 importance of co-precipitation. *Open Environ. J.* 1 (2007), 9-13.
- 409 [21] C. Noubactep, A critical review on the mechanism of contaminant removal in Fe⁰-H₂O
410 systems. *Environ. Technol.* 29 (2008), 909-920.

411 [22] M.J. Mura, S. Behr, E.F. Bres, J.C. Voegel, Dynamic processes at the liquid/solid
412 interface in the albumin/apatite system. *Clin. Mater* 5 (1990), 285-295.

413 [23] K.S. Geetha, G.D. Surender, Solid-liquid mass transfer in the presence of micro-particles
414 during dissolution of iron in a mechanically agitated contactor. *Hydrometallurgy* 36 (1994),
415 231-246.

416 [24] P. Polasek, Differentiation between different kinds of mixing in water purification – back
417 to basics, *Water SA* 33 (2007), 249-252.

418 [25] C.S. André, M. Khraisheh, Removal of humic substances from drinking water using
419 GAC and iron-coated adsorbents: Consideration of two kinetic models and the influence of
420 mixing. *Environ. Eng. Sci.* 26 (2009), 235-244.

421 [26] N.D. Tomashov, L.P. Vershinina, Kinetics of some electrode processes on a continuously
422 renewed surface of solid metal. *Electrochim. Acta* 15 (1970), 501-517.

423 [27] A.T. Corey, B.W. Auvermann, Transport by Advection and Diffusion Revisited. *Vadose*
424 *Zone Journal* 2 (2003), 655-663.

425 [28] A.T. Corey, S.D. Logsdon, Limitations of the chemical potential. *Soil Sci. Soc. Am. J.* 69
426 (2005), 976-982.

427 [29] Potgieter J.H., Adsorption of methylene blue on activated carbon: An experiment
428 illustrating both the Langmuir and Freundlich isotherms. *J. Chem. Educ.* 68 (1991), 349-350.

429 [30] Avom J., J. Ketcha, C. Noubactep, P. Germain, Adsorption of methylene blue from an
430 aqueous solution onto activated carbons from palm-tree cobs. *Carbon* 35 (1997), 365-369.

431 [31] A.A. Attia, B.S. Girgis, N.A. Fathy, Removal of methylene blue by carbons derived from
432 peach stones by H₃PO₄ activation: Batch and column studies. *Dyes and Pigments* 76 (2008),
433 282-289.

434 [32] B.D. Jones, J.D. Ingle, Evaluation of redox indicators for determining sulfate-reducing
435 and dechlorinating conditions. *Water Res.* 39 (2005), 4343-4354.

436 [33] V. Ender, Zur Struktur der Phasengrenze Metalloxid/Elektrolyt-Potentialbildung und
437 Ladungsbilanz. *Acta Hydrochim. Hydrobiol.* 19 (1991), 199-208.

438 [34] J.E. Post, Manganese oxide minerals: Crystal structures and economic and environmental
439 significance. *Proc. Natl. Acad. Sci. USA* 96 (1999), 3447-3454.

440 [35] C. Noubactep, G. Meinrath, J.B. Merkel, Investigating the mechanism of uranium
441 removal by zerovalent iron materials. *Environ. Chem.* 2 (2005), 235-242.

442 [36] C. Noubactep, Characterizing the Discoloration of Methylene Blue in Fe^0/H_2O Systems.
443 *J. Hazard. Mater.* (2009), (Accepted).

444 [37] C. Mbudi, P. Behra, B. Merkel, The Effect of Background Electrolyte Chemistry on
445 Uranium Fixation on Scrap Metallic Iron in the Presence of Arsenic. Paper presented at the
446 Inter. Conf. Water Pollut. Natural Porous Media (WAPO2), Barcelona (Spain) April 11 – 13
447 (2007), 8 pages.

448 [38] Kurth A.-M.F., Discoloration of Methylene Blue by Elemental Iron - Influence of the
449 Shaking Intensity. Bachelor Thesis, University of Göttingen (Germany) (2008) 36 pages.

450 [39] R.P. Buck, S. Rondinini, A.K. Covington, F.G.K. Baucke, C.M.A. Brett, M.F. Camoes,
451 M.J.T. Milton, T. Mussini, R. Naumann, K.W. Pratt, P. Spitzer, G.S. Wilson, Measurement of
452 pH. Definition, standards, and procedures (IUPAC Recommendations 2002), *Pure Appl.*
453 *Chem.* 74 (2002), 2169-2200.

454 [40] D.F.A. Koch, Kinetics of the reaction between manganese dioxide and ferrous ion. *Aust.*
455 *J. Chem* 10 (1957), 150-159.

456 [41] D. Postma, C.A.J. Appelo, Reduction of Mn-oxides by ferrous iron in a flow system:
457 column experiment and reactive transport modelling. *Geochim. Cosmochim. Acta* 64 (2000),
458 1237-1247.

459 [42] B.K. Lavine, G. Auslander, J. Ritter, Polarographic studies of zero valent iron as a
460 reductant for remediation of nitroaromatics in the environment. *Microchem. J.* 70 (2001), 69-
461 83.

- 462 [43] Z. Hao, X. Xu, J. Jin, P. He, Y. Liu, D. Wang, Simultaneous removal of nitrate and
463 heavy metals by iron metal, *J. Zhejiang Univ. Sci.* 6B (2005), 353-356.
- 464 [44] W.S. Pereira, R.S. Freire, Azo dye degradation by recycled waste zero-valent iron
465 powder. *J. Braz. Chem. Soc.* 17 (2006), 832-838.
- 466 [45] M.L. de Vries, I.E. Grey, Influence of pressure on the kinetics of synthetic ilmenite
467 reduction in hydrogen. *Metal. Mater. Trans. B* 37B (2006), 199-208.
- 468

468 **Table 1:** Characteristics, surface coverage and function of the individual reactive materials of
 469 this study. Apart from Fe⁰ the given value of specific surface area (SSA) for are the
 470 minima of reported data. The point of zero charge (pH_{pzc}) for all materials is lower
 471 than the initial pH value. Therefore, MB adsorption onto the negatively charged
 472 surfaces is favorable. The surface coverage is estimated using the method presented
 473 by Jia et al. [18]. The total surface that can be covered by the amount of MB present
 474 in 22 mL of a 0.037 mM is S_{MB} = 0.997 m². Modified after Noubactep [36].
 475

System	pH _{pzc}	SSA (m ² g ⁻¹)	S _{available} (m ²)	Coverage (-)	Function
Fe ⁰	7.6	0.29	0.032	18.8	MB co-precipitant
Fe ⁰ + MnO ₂	-	-	4.432	0.13	-
MnO ₂	2.0 - 6.0	40	4.4	0.14	delays CP availability
GAC	7.0 - 8.0	200	22	0.03	MB adsorbent
Fe ⁰ + GAC	-	(-)	22.032	0.03	-

476

477

477 **Table 2:** Overview on the investigated systems with the predicted and observed effects of
 478 mixing on their behaviour.

System	Composition	Expected effect of the material(s)	Predicted mixing effects	Observed mixing effects
I	Fe ⁰	MB co-precipitation	scouring	suspension of Fe-oxides
II	GAC	MB adsorption	attrition	increased adsorption
III	MnO ₂	MB adsorption	attrition	increased adsorption
IV	Fe ⁰ , GAC	increased MB discoloration	unknown	adsorption and co-precipitation
V	Fe ⁰ , MnO ₂	decreased MB discoloration	unknown	adsorption and co-precipitation

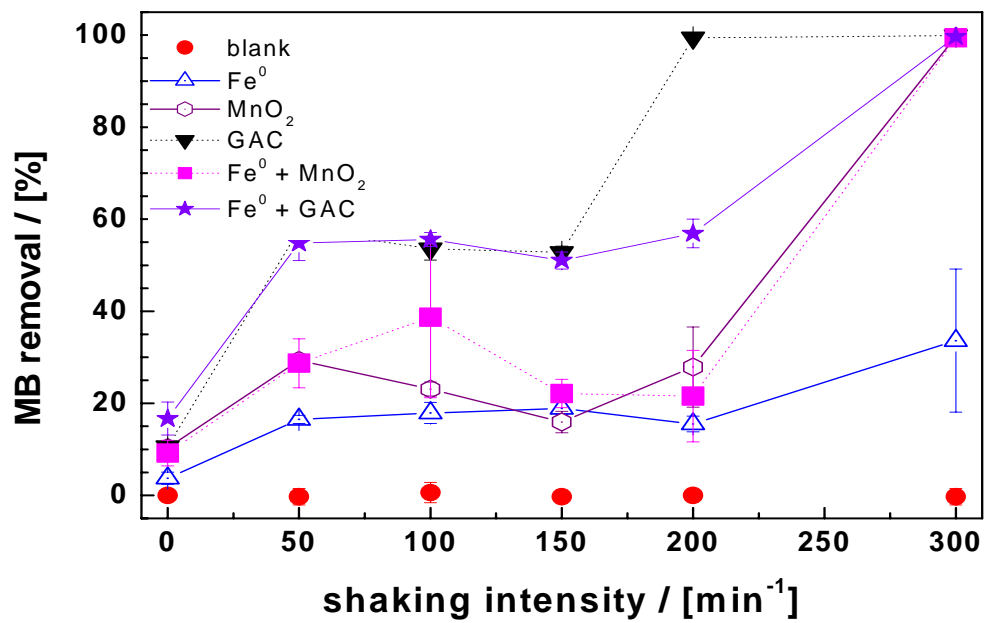
479

480

481

482

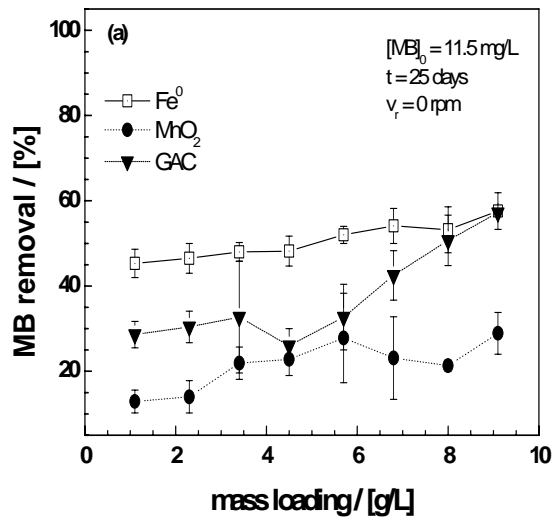
482 **Figure 1**



483

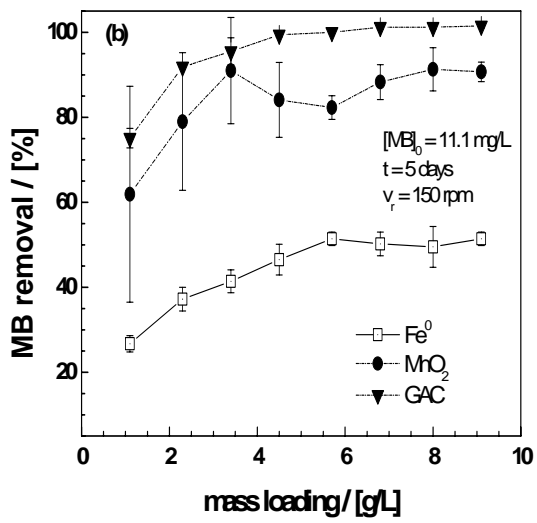
484

484 Figure 2



485

486



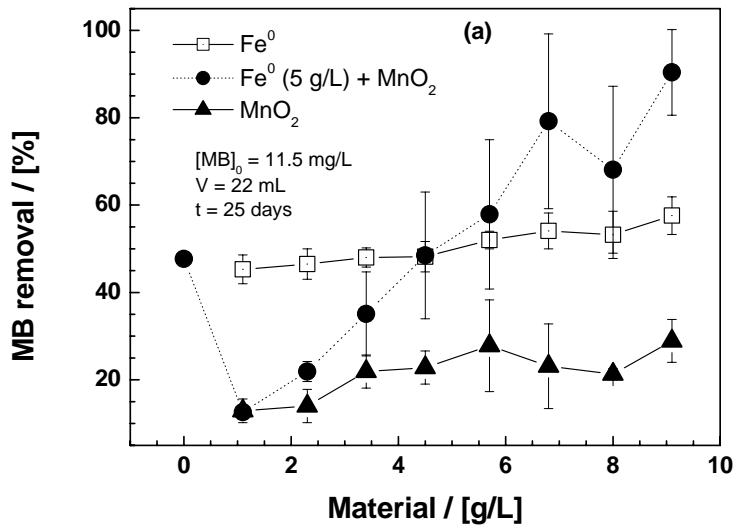
487

488

489

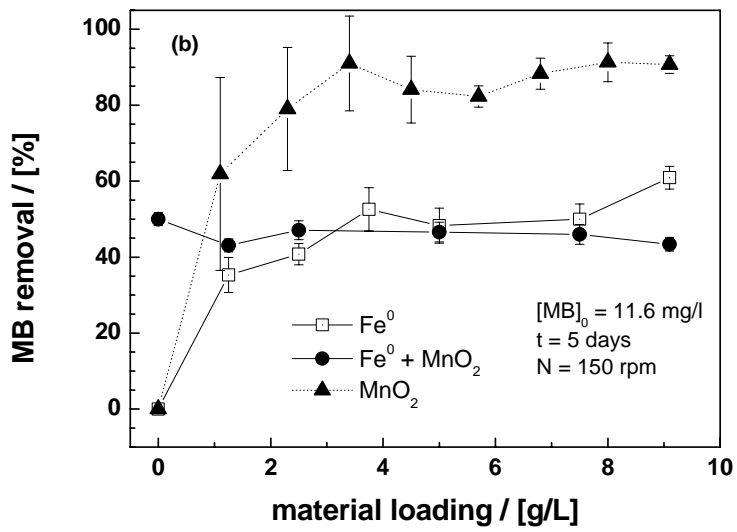
489 **Figure 3**

490



491

492

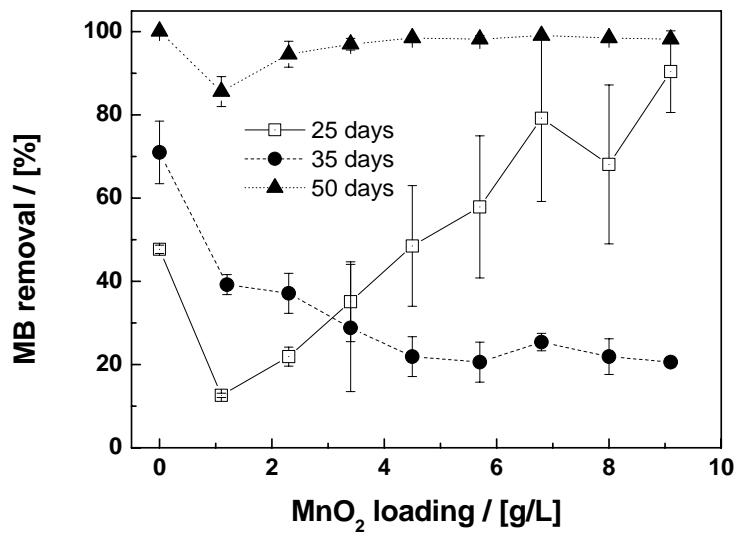


493

494

495

495 **Figure 4**



496

497

498

498 **Figure Captions**

499

500 **Figure 1:** Methylene blue discoloration in all five systems for 24 hours as a function of the
501 shaking intensity. The lines are not fitting functions, they simply connect points to facilitate
502 visualization.

503 **Figure 2:** Methylene blue discoloration by the individual materials under non-disturbed
504 conditions (a) and at a shaking intensity of 150 min^{-1} (b). The lines are not fitting functions,
505 they simply connect points to facilitate visualization.

506 **Figure 3:** Methylene blue discoloration by Fe^0 as influenced by the presence of MnO_2 in non-
507 disturbed experiments for 25 days (a) and experiments shaken at 150 min^{-1} for 5 days. the
508 individual materials und non-disturbed conditions for 25 days. The lines are not fitting
509 functions, they simply connect points to facilitate visualization.

510 **Figure 4:** Comparison of the extent of MB discoloration by Fe^0 (5 g/l) as influenced by the
511 MnO_2 mass loading in non-disturbed experiments for 25, 35 and 50 days. It can be seen than
512 if the experiments were performed only for 50 days, neither the redox indicator properties of
513 MB (25 days) nor the delay in MB discoloration in the presence of MnO_2 (25 and 35 days)
514 could be evidence (see text). It can be emphasized that, when using various Fe^0 mass
515 loadings, mixing devices and reaction times, investigators have studies different processes
516 and compared them to each other. The experiment for 35 days were performed with 20 mg/l
517 MB [36]. The lines are not fitting functions, they simply connect points to facilitate
518 visualization.

519

519 **Supplementary Content**

520 **Evidence for the effect of shaking on the process MB discoloration**

521 Figure SC1 shows the photographs of essay tubes containing all investigated systems in two
522 experiments performed at a shaking intensity of 300 min^{-1} . The duration of the experiments
523 were one and three days. The photographs show clearly that shaking at 300 min^{-1} induces
524 suspension of Fe^0 and MnO_2 dissolution products. The photographs presented in Fig. 1 were
525 made one week after the end of the experiments. Immediately at the end of the experiment,
526 suspended fines could be observed in the essay tubes containing GAC alone, showing that the
527 vibration induced by this shaking intensity was sufficient to produce fines from a chemically
528 inert material (GAC). At this shaking intensity, the expected lower MB discoloration in
529 system V ($\text{Fe}^0 + \text{MnO}_2$) relative to system I (Fe^0 alone) could not be observed. Therefore,
530 assumption 1 (*Assumption 1: any shaking intensity relevant for natural situations should*
531 *solely speed up processes observed under non-disturbed conditions*) is not verified suggesting
532 that a shaken intensity of 300 min^{-1} is too high to be relevant for natural situations. Natural
533 situations are mostly characterized be diffusion-controlled processed.

534

534 **Figure SC1**

535



536

537 **Figure SC1:** Photographs of shaken assay tubes containing from the left to the right: no

538 additive (blank), Fe^0 alone, MnO_2 alone, GAC alone, $\text{Fe}^0 + \text{MnO}_2$ and $\text{Fe}^0 +$

539 GAC. The assay tubes were shaken for 3 days (up) and 1 day (bottom). The

540 photographs were made one week after the end of shaking operations.